Arginine deprivation alters DNA damage response in arginosuccinate synthetase negative glioblastoma and potentiates standard of care

Avik Ghosh[1,2], Richard Perryman[1] Kevin O'Neill[1], Nelofer Syed[1]

[1]John Fulcher Molecular Neuro-oncology Laboratory, Department of Brain Sciences, Imperial College, London, UK [2] Department of Surgery and Cancer, Imperial College London, UK

Email Correspondence: avik.ghosh18@imperial.ac.uk

Background

Glioblastoma (GBM) is both the most prevalent and aggressive primary brain malignancy. Its poor clinical prognosis lies partly in its vast intra and intertumoural heterogeneity, the inability of many drugs to pass the blood brain barrier and its upregulation of DNA repair pathways thus rendering treatment resistance to standard of care; surgical resection, temozolomide and radiotherapy [1-3]. Arginine deprivation by ADI-PEG20 provides a novel metabolic approach to this issue, targeting GBM cells with an inability to produce their own arginine due to transcriptional loss (methylation) of arginosuccinate synthetase 1 (*ASS1*). ADI-PEG20 peripherally depletes serum levels of arginine leading to regression of tumour growth in xenograft models, overcoming problems posed by blood brain barrier passage [4]. We have previously shown that *ASS1* negative GBM has poorer survival, however, the mechanism behind this remains unclear [5]. The role of DNA repair in GBM is well established in context of intrinsic therapeutic efficacy and acquired resistance [6]. We aimed to investigate a potential association between DNA damage repair and ADI-PEG20 treatment in *ASS1* negative GBM. We hypothesise that poorer prognosis is attributed to enhanced DNA repair in ASS1 negative GBM, and that ADI-PEG20 will synergise with current therapies.

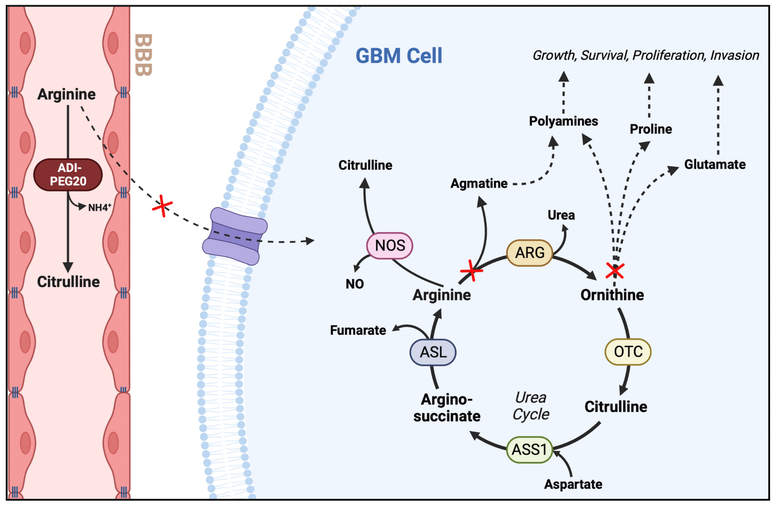

Figure 1: Shows the important components of the Urea cycle, its metabolites and key enzymes. Abbreviations: **ASS1** – Arginosuccinate Synthetase 1, **ASL** – Arginosuccinate Lyase, **ARG** – Arginase, **OTC** – Ornithine Transcarboxylase, **NOS** – Nitric Oxide Synthase, **NO** – Nitric Oxide. The red X's mark the metabolic consequences of ADI-PEG20 which involves peripheral conversion of arginine to citrulline. In ASS1 negative tumours this means citrulline accumulates and polyamine, proline and glutamate levels decrease reducing malignant phenotype progression therefore preventing growth, survival, proliferation and invasion. Adapted from Mörén et al 2018 using Biorender

Methodology

SRB Proliferation Assay

With the primary cell line GBM31, naturally ASS1 negative, we investigated the effect of 1µg/ml ADI-PED20 in combination with current therapies on proliferation compared to an ASS1 overexpressing GBM31 cell line. A Sulforhodamine B colorimetric assay was used to quantify optical density (cell mass) at day 0, 3 and 6 of treatment thus indirectly measuring proliferation with different treatment combinations. ASS1 fold change in expression was confirmed in empty vector and transfected cell lines with RT-qPCR using the $2^{-\Delta\Delta Ct}$ method.

QIAGEN RT² Profiler™ Array

Triplicates of GBM31 and GBM96 (ASS1 negative lines) were plated and treated with and without ADI-PEG20 for 24 hours followed by RNA extraction using QIAGEN RNeasy kits. cDNA synthesis and genomic DNA elimination was performed using the QIAGEN RT² First Strand kits. The catalogued RT² Profilers for human DNA repair were used (PAHS-042Z) to quantify RNA expression of pathway specific genes in the samples. Three biological repeats were performed.

Statistical Analysis

Performed using GraphPad Prism v9.0 and the online QIAGEN GeneGlobe analysis tool.

Results

Transfected GBM31 Overexpresses *ASS1*

Fold expression of *ASS1* between the transfected line GBM31-ASS1 and an empty vector control was quantified using basic qPCR (Figure 2). As expected, there was a 52-fold increase in expression in the overexpressing line (p=0.0027). ASS1 expression was low in the empty vector control, we refer to this as ASS1 negative.

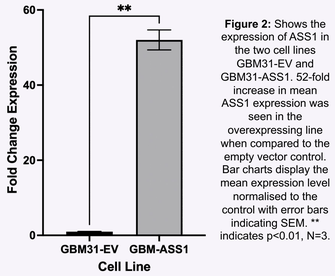

Figure 2: Shows the expression of ASS1 in the two cell lines GBM31-EV and GBM31-ASS1. 52-fold increase in mean ASS1 expression was seen in the overexpressing line when compared to the empty vector control. Bar charts display the mean expression level normalised to the control with error bars indicating SEM. ** indicates p<0.01, N=3.

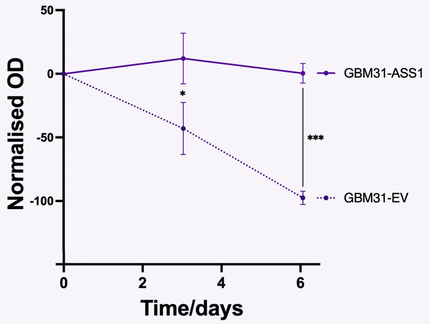

Figure 3: Shows response to ADI-PEG20 in the two separate cell lines normalised to the citrulline control for each corresponding day. Error bars represent the standard deviation of datasets. * Indicates p<0.05,*** indicates p<0.001

Low ASS1 Expression Correlates with Increased Susceptibility to ADI-PEG20

Figure 3 shows the proliferation of ADI-PEG20 treated GBM31-EV (ASS1 negative) and GBM31-ASS1 (ASS1 positive) cells normalised to the control. Unpaired t-test revealed significant decreased expression as early as day 3 (p=0.029) in the ASS1 negative cell line. Day 6 showed more significant decrease in proliferation (p=0.0001). This demonstrated the susceptibility of GBM31 to ADI-PEG20.

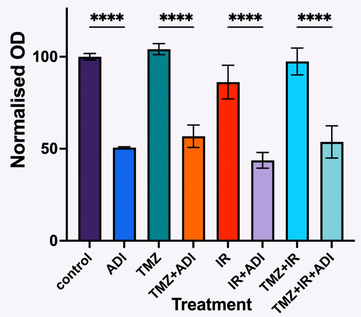

Figure 4: Response of the ASS1 negative GBM31 empty vector control to different treatment combinations seen on the x axis. Bar charts represent the optical density, proportional to the proliferation, normalised to the control. Error bars represent the standard deviation of the datasets. **** indicates p<0.0001

ADI-PEG20 has an Additive Effect with Current Therapy

Figure 4 shows day 6 proliferation upon addition of ADI-PEG20 to different combinations of standard treatment in the empty vector control. One-way ANOVA revealed highly significant decreases in proliferation in all ADI-PEG20 treated groups with lowest the proliferation noted in the ADI-PEG20 and irradiation group.

Addition of ADI-PEG20 Alters the Expression Profile of DNA Repair Genes in ASS1 Negative Cell Lines

Following these initial experiments, expression of DNA repair genes were analysed using QIAGEN RT² Profilers on the primary cell lines GBM96 and GBM31, both with low ASS1 expression, treated with ADI-PEG20. Figure 5 shows the clustergram analysis of this RNA expression data, revealing distinct expression profiles between control and treatment groups. GBM31 showed less extensive changes than GBM96. Pooled analysis revealed significant downregulation of *BRIP1* (-2.09 fold, p = 0.0104), *LIG1* (-2.56 fold, p = 0.0212) and *DMC1* (-2.2 fold, p = 0.0497).

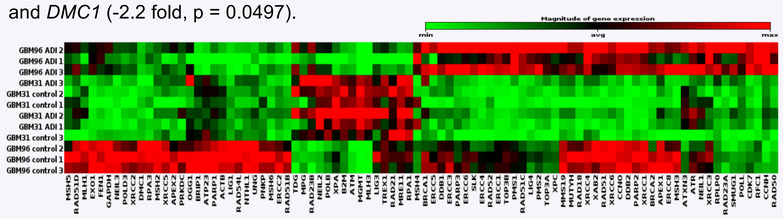

Figure 5: Heatmap showing the expression of 84 key genes involved in base excision, nucleotide excision, mismatch, single and double strand break repair. The focussed set of genes are listed on the bottom. Expression was analysed in 12 samples shown on the left hand side, 3 biological repeats in GBM31 and GBM31 both with and without 24 hours of treatment with ADI-PEG20. The expression intensities key is shown on the top right hand side with red indicating maximum gene expression (upregulation) and green indicating the minimum gene expression (downregulation). A detailed image of the Clustergram can be found by scanning the QR code found at the end of the poster*

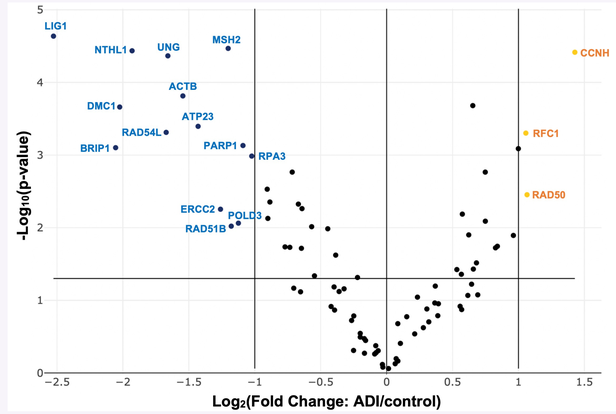

Figure 6: The volcano plot of the DNA repair gene expression profile of GBM96 is shown with Log_2(fold change) shown on the x axis. The p value threshold for significance was set at 0.05 (horizonal black line). The blue dots represent the DNA repair genes that were significantly downregulated (>2 fold), for ease of presentation they have been labelled corresponding to the relevant genes. The yellow dots represent the upregulated DNA repair genes (>2 fold), they have been labelled with orange text. The black dots represent the DNA repair genes that were not significantly upregulated or downregulated, they have not been labelled for simplicity. This plot was generated using the QIAGEN GeneGlobe Online Analysis Tool

ADI-PEG20 Treatment is Predominantly Associated with Downregulation of Key DNA Repair Genes in GBM96

Analysis of GBM96 was done separately and yielded the volcano plot seen in Figure 6. The differentially expressed genes have been labelled. 14 genes were found to be significantly downregulated upon ADI-PEG20 treatment when compared to the control group (p<0.05). In addition to the genes identified in the Clustergram, *RAD51B, PARP1, ATP23, MSH2, UNG* and *NTHL1* genes were amongst those that were significantly downregulated. Interestingly, *RFC1*, *CCNH* and *RAD50* genes appear to be upregulated significantly upon ADI-PEG20 treatment.

Conclusions

- Low expression of ASS1 correlates with sensitivity to ADI-PEG20, which is efficacious in combination with radiation, as shown by others in spheroid models[7]
- In ASS1 negative GBM, treatment with ADI-PEG20 leads to significant downregulation of genes involved in DNA repair"
- **Possible mechanisms**: ADI-PEG20 downregulates DNA repair mechanisms leading to enhanced DNA damage by DNA damaging agents
  - Much literature on inhibition of DNA repair proteins enhancing cytotoxicity [8]
  - LIG1 overexpression correlates with treatment resistance and poorer survival [9]
  - Inhibition of RAD51 has been shown to radiosensitise GBM[10]

Future Directions

- Further validation at the proteomic level is needed
- Validate individual gene expression in both ASS1 negative and positive cells
- Novel therapeutic combinations can be explored; LIG1 inhibitors or Olaparib
- Further in-vivo experiments using ADI-PEG20 in combination with radiation on low *ASS1* expressing xenograft models

References

1. Ostrom QT, Gittleman H, Truitt G, Boscia A, Kruchko C, Barnholtz-Sloan J. CBTRUS Statistical Report: Primary Brain and Other Central Nervous System Tumors Diagnosed in the United States in 2011–2015. *Neuro-oncology (Charlottesville, Va.)*; *Neuro Oncol.* 2018; 20 iv1-iv86. 10.1093/neuonc/noy131.
2. Ohka F, Natsume A, Wakabayashi T. Current trends in targeted therapies for glioblastoma multiforme. *Neurology Research International.* 2012; 2012 878425. 10.1155/2012/878425.
3. Stupp R, Dr, Hegi ME, PhD., Mason WP, M.D., van den Bent, Martin J, MD, Taphoorn MJB, Janzer RC, M.D., et al. Effects of radiotherapy with concomitant and adjuvant temozolomide versus radiotherapy alone on survival in glioblastoma in a randomised phase III study: 5-year analysis of the EORTC-NCIC trial. *The lancet oncology; Lancet Oncol.* 2009; 10 (5): 459-466. 10.1016/S1470-2045(09)70025-7.
4. Przystal JM, Hajji N, Khozoie C, Renziehausen A, Zeng Q, Abaitua F, et al. Efficacy of arginine depletion by ADI-PEG20 in an intracranial model of GBM. *Cell Death & Disease.* 2018; 9 (12): 1192. 10.1038/s41419-018-1195-4.
5. Syed N, Langer J, Janczar K, Singh P, Lo Nigro C, Lattanzio L, et al. Epigenetic status of argininosuccinate synthetase and argininosuccinate lyase modulates autophagy and cell death in glioblastoma. *Cell Death & Disease.* 2013; 4 (1): e458. 10.1038/cddis.2012.197.
6. Bonm A, Kesari S. DNA Damage Response in Glioblastoma: Mechanism for Treatment Resistance and Emerging Therapeutic Strategies. *Cancer Journal (Sudbury, Mass.).* 2021; 27 (5): 379-385. 10.1097/PPO.0000000000000540.
7. Hinrichs CN, Ingargiola M, Käubler T, Löck S, Temme A, Köhn-Luque A, et al. Arginine Deprivation Therapy: Putative Strategy to Eradicate Glioblastoma Cells by Radiosensitization. *Molecular Cancer Therapeutics.* 2018; 17 (2): 393-406. 10.1158/1535-7163.MCT-16-0807.
8. Ferri A, Stagni V, Barilà D. Targeting the DNA Damage Response to Overcome Cancer Drug Resistance in Glioblastoma. *International journal of molecular sciences; Int J Mol Sci.* 2020; 21 (14): 4910. 10.3390/ijms21144910.
9. Ali R, Alabdullah M, Algethami M, Albilhy A, Miligy I, Shoqafi A, et al. Ligase 1 is a predictor of platinum resistance and its blockade is synthetically lethal in XRCC1 deficient epithelial ovarian cancers. *Theranostics; Theranostics.* 2021; 11 (17): 8350-8361. 10.7150/thno.51456.
10. King HO, Brend T, Payne HL, Wright A, Ward TA, Patel K, et al. RAD51 Is a Selective DNA Repair Target to Radiosensitize Glioma Stem Cells. *Stem Cell Reports.* 2017; 8 (1): 125-139. https://doi.org/10.1016/j.stemcr.2016.12.005.

*Scan this QR code: to see the full version of figure 5 with hierarchical clustering